DEVELOPMENTS in Optics and Communications 2021

# DOC 2021

## 17th INTERNATIONAL YOUNG SCIENTIST CONFERENCE

# ABSTRACT BOOK

**CONFERENCE TOPICS:**

Biophotonics
Laser Physics and Spectroscopy
Vision Science
Optical Materials and Phenomena

**WWW.DOCRIGA.LV**

SPIE. STUDENT CHAPTER UNIVERSITY OF LATVIA

OSA University of Latvia Student Chapter

UNIVERSITY OF LATVIA

# DOC 2021 Abstract Book

17th International Young Scientist conference
*Developments in Optics and*
*Communications 2021*

Editor: Inga Brice
Institute of Atomic Physics and Spectroscopy
University of Latvia
Jelgavas street 3, Riga, LV1004,Latvia

ISBN 978-9934-23-356-2



Cover design: Nellija Lace, Inga Brice

www.docriga.lv

# Welcome

Dear participants of **DOC 2021**,

The **DOC 2021** conference (April 15-16) is organized jointly by University of Latvia SPIE student chapter, OSA Latvian student chapter and University of Latvia. The purpose of this conference is to bring together students and young scientists working experimentally and theoretically in the fields of optics and photonics to share and exchange new ideas and to establish contacts for future collaboration.

Best regards,
DOC 2021 Organizers

# The Organizing Committee

## DOC chairs

- Inga Brice
  PhD student, research assistant
  University of Latvia
- Ilze Oshina
  PhD student, researcher
  University of Latvia

## Organizers

- Zane Jansone-Langina
- Kristine Kalnica Dorosenko
- Tatjana Pladere
- Lasma Asare

## Scientific committee

- Prof. Ruvin Ferber
  Faculty of Physics and Mathematics, University of Latvia
- Dr. Varis Karitans
  Department of Optometry and Vision science, University of Latvia
- Prof. Uldis Rogulis
  Institute of Solid State Physics, University of Latvia
- Prof. Janis Spigulis
  Institute of Atomic Physics and Spectroscopy, University of Latvia

# Contents

## Invited Speakers



## Talks

Laser Physics and Spectroscopy

Optical Materials and Phenomena



Biophotonics

# Poster Session 1

# Poster Session 2

# Part I
# Invited Speakers

# Electron magnetic resonance in optical materials

Antuzevics Andris

*Institute of Solid State Physics, University of Latvia*

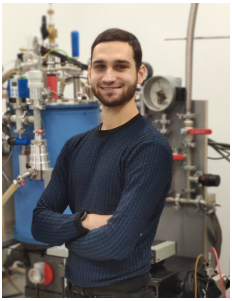

Point defects are ubiquitous in solids and play a crucial role in their mechanical, chemical, thermal, electrical, magnetic and optical properties. A common strategy for tailoring the performance of materials is via introduction of foreign ions (activators). Methods of defect and impurity ion identification, characterization and quantification are, therefore, of high fundamental and practical interest.

Electron paramagnetic resonance (EPR) spectroscopy encompasses a set of techniques, which are valuable for the investigations of materials possessing unpaired electrons. In this talk general aspects of EPR spectroscopy will be explained with a focus on applications in optical materials. Examples will be given on the characterization of luminescent glass ceramics, persistent phosphors, photochromic materials, X-ray irradiated glasses and functional materials relevant to fusion reactors. Principles and applications of optical detection of magnetic resonance (ODMR) techniques will also be covered.

**Acknowledgments**

The financial support of Latvian Council of Science grant LZP-2018/1-0335 “Novel transparent nanocomposite oxyfluoride materials for optical applications” is greatly acknowledged.

# Sculpting the light with reconfigurable meta-optics

Shalaginov Mikhail Y.

*Massachusetts Institute of Technology, Department of Materials Science and Engineering (Cambridge, MA, USA)*

*E-mail:* mys@mit.edu

The ability to reconfigure an optical component has been a Holy grail for optical engineers. Traditionally, it requires bulky mechanical moving parts, for example in a zoom lens. This optical architecture comes with the price of increased size and complexity, which further leads to limited speed and ruggedness. Unlike conventional optics which rely on geometric curvature to mold the propagating light, metasurfaces afford on-demand control of a wavefront using subwavelength antenna arrays patterned via standard planar microfabrication technologies [1]. In addition to their benefit of significantly reduced form-factor, they also present a versatile suite of solutions to realizing tunable optical systems, also termed as "active metasurfaces". A variety of non-mechanical tuning mechanisms, such as free-carrier, thermo-optic, electro-refractive phenomena and others, have been harnessed. However, demonstrated meta-optical devices incur either narrow tuning ranges or low optical efficiencies.

Is it still possible to build a high-performance non-mechanically actuated metasurface?

In this talk, I will present our team's approach to address this challenge by leveraging the combined material and design innovation. On materials side, we have developed a new non-volatile chalcogenide alloy $Ge_2Sb_2Se_4Te_1$ (further termed as GSST) exhibiting giant index contrast ($^{\circ}n > 1.5$) and unique broadband transparency in infra-red for both amorphous and crystalline states [2]. GSST claims an exceptional phase-change material with a figure-of-merit exceeding by two orders of magnitude that of the traditional $Ge_2Sb_2Te_5$ alloy. On the optical design front, we pioneered a design principle enabling binary switching of metasurfaces between arbitrary phase profiles, which is further scalable to multi-state switching. Based on the material and design advances, our group demonstrated a mid-infrared varifocal metalens, that features 1) aberration-free performance across arbitrary optical states; 2) unprecedentedly low crosstalk, characterized by a record contrast ratio of nearly 30 dB; and 3) considerably enhanced focusing efficiency exceeding 20% in both states [3]. We applied the active metalens to demonstrate crosstalk-free multi-depth imaging of objects with diffraction-limited resolution. While our device architecture and design principle are generic to active metasurfaces across different wavelength ranges, this demonstration also fills in a technological gap as a high-performance active metalens for imaging applications in the strategically important mid-IR waveband. At the end I will discuss the potential avenues to further advance reconfigurable metasurfaces, particularly via more sophisticated design and optimization

approaches [4].

**References**

[1] P. Lalanne and P. Chavel, "Metalenses at visible wavelengths: past, present, perspectives," Laser Photon. Rev. 11, 1600295 (2017).

[2] Y. Zhang, J. B. Chou, J. Li, H. Li, Q. Du, A. Yadav, S. Zhou, M. Y. Shalaginov, Z. Fang, H. Zhong, C. Roberts, P. Robinson, B. Bohlin, C. Ríos, H. Lin, M. Kang, T. Gu, J. Grossman, J. Warner, V. Liberman, K. Richardson, J. Hu, "Broadband transparent optical phase change materials for high-performance nonvolatile photonics", Nature Communications, 10, 1, 1-9 (2019).

[3] M. M. Y. Shalaginov, S. An, Y. Zhang, F. Yang, P. Su, V. Liberman, J. B. Chou, C. M. Roberts, M. Kang, C. Rios, Q. Du, C. Fowler, A. Agarwal, K. Richardson, C. Rivero-Baleine, H. Zhang, J. Hu, T. Gu, "Reconfigurable all-dielectric metalens with diffraction limited performance", Nat. Commun. 12, 1225, 1-8 (2021).

[4] M. Y. Shalaginov, S. An, Y. Zhang, S. D. Campbell, F. Yang, C. Ríos1, L. Kang, D. H. Werner, H. Zhang, J. Hu, T. Gu, "Design for quality: reconfigurable flat optics based on active metasurfaces", Nanophotonics, 9, 3505–3534 (2020).

# Biophotonics for animal health

Cugmas Blaz

*University of Latvia, Institute of Atomic Physics and Spectroscopy*

In this presentation, we introduced veterinary medicine and analyzed the potential of biophotonics and biomedical optics for animal health.

Veterinary medicine handles non-human aspects of medicine, including preventive, diagnostic and, therapeutic procedures on companion and farm animals. As in humans, medicine in companion animals (e.g., dogs, cats, horses) is personalized since pets present a psychological and social value to owners. Farmed animals exhibit mainly monetary value; therefore, the veterinary services are normally preventive and depend on the animal value. Monitoring animal-origin food (e.g., meat, dairy, eggs) quality and safety is another important veterinary aspect.

Promising optical techniques such as optical coherence tomography, pulse oximeter, and hyperspectral imaging have been clinically translated into human medicine. However, biophotonics remains rarely exploited in companion animals. There are some biophotonics studies in veterinary oncology which addressed tumor diagnosis (skin and subcutaneous tumors), prognosis (lymphoma), and therapy (clear surgical margins). Visible and near-infrared spectroscopy served for measuring various physiological parameters related to circulation. Photobiomodulation therapy was often used to manage wounds, skin conditions, and orthopedic problems in dogs and horses. The future veterinary optical devices should be robust and resilient to damage (e.g., due to biting, chewing), offering user-friendly and short measurements. In veterinary oncology, biophotonics could replace an invasive fine-needle aspiration procedure. The potential of a pulse oximeter for pet monitoring has yet to be explored. What is more, photobiomodulation efficiency should be tested in an extensive clinical (in vivo) study. The technique would be very beneficial in dentistry which currently requires expensive and risky anesthesia.

# Presbyopic madness

Solomatin Andrei

Presbyopia is a global problem, affecting billion people worldwide. This condition is inevitable for humans reaching 40-45 years of age. Today, presbyopia is a "holy grail" in ophthalmology and a lot of effort is made in the industry to tackle this condition.

**What is presbyopia?** Today, there is no straightforward explanation for presbyopia. The definition is equivocal and most theories support Helmholtz's theory (1821-1894). From my point of view most precise definition is given by Dr.J.S.Wolffsohn and Dr.L.N.Davies "presbyopia occurs when the physiologically normal age-related reduction in the eye's focusing range reaches a point, when optimally corrected for distance vision, that the clarity of vision at near is insufficient to satisfy an individual's requirements".

**How presbyopia is managed today?** In 2021 there are multiple presbyopia correction modalities. Non surgical correction options are, spectacles (single vision, bifocal/trifocals, progressive lenses), contact lenses (monovision, multifocal lenses). But still, using this type of correction dynamic accommodation is not restored and patient is still spectacle or lens dependant. Nowadays more effective, but also more risky option is surgical approach, it gives spectacle independence and can satisfy patients, who are more demanding to preserve active lifestyle.

Most popular surgical methods are; laser refractive treatment and refractive lens exchange. Laser refractive corneal surgery is not permanent solution, because it change corneal refractive power without changing any lens functions. So for today, one may say "golden standard", in permanent presbyopia treating modalities is refractive lens exchange with artificial IOL.

There are many options today: monovision, multifocal IOL, extended depth of focus lenses, hybrid IOL. But all the modern multifocal lenses despite of the design, either fresnel diffractive design, or by indusing spherical aberration, do have a problem of light scattering and inducing dysphotopsia symptoms.

To battle this problem industry come up with new accommodating IOL designs, some of which are in the clinical trial process (Fluid Vision IOL, Synchrony IOL, Juvene, Lumina, ATIA vision IOL).

Despite many options that industry have today, presbyopia is still a challenge in ophthalmology and best solution is yet to come.

# SimVis Gekko Visual Simulator: a novel ophthalmic instrument developed from scratch

Barcala Xoana[1,2]

[1] *PhD Candidate at Visual Optics and Biophotonics Lab & 2EyesVision*

[2] *Clinical Developer at 2EyesVision*

Presbyopia, the loss of the ability to focus near objects, affects 100% of the population over 45 years old. The use of ophthalmic corrections based on simultaneous vision, that provide vision in focus for far and near objects at the same time, is increasing, in the form of multifocal intraocular lenses (M-IOLs) replacing the crystalline lens, or contact lenses (CLs) added to the cornea. Due to the high number of multifocal designs available, the enormous difficulty to describe multifocal vision to the patient, it is challenging toto select the best correction for each patient, one of the reasons for an increasing demand for visual simulators.

Visual simulators, initially developed in research laboratories, are designed to simulate the through focus optical quality of multifocal solutions, so the subject can experience the corrections before surgery. Most visual simulators are based on adaptive optics (AO) elements (deformable mirrors or spatial light modulators) where a phase pattern representing a given lens is mapped. However, they are expensive and very sophisticated.

SimVis Gekko (2EyesVision, Madrid) is the first binocular simultaneous vision see-through simulator, wearable, with a wide field of view (¿20°), designed for its use in the clinic. It simulates multifocal corrections using tunable lenses working under temporal multiplexing. Temporal multiplexing is based on fast periodic optical power variations at speeds greater than the defocus flicker fusion of the human visual system, generating on the patient's retina multifocal images that are apparently static and programmable.

A review of how the SimVis Gekko was developed and characterized from scratch, and its clinical validations will be presented.

# Studying vision using Adaptive Optics based visual simulators

Vinas-Pena Maria

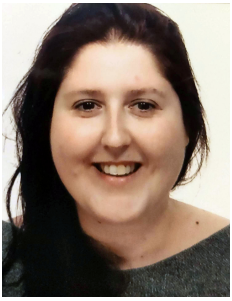

The optical projection of images of the outside world onto the retina is the first step in the visual process. However, the human eye is far from being a perfect optical system, and, as a consequence, the images projected on the retina are blurred by ocular aberrations, as well as diffraction and scattering. They impose the first limit to spatial vision, generally reducing contrast and the spatial frequency content that is transmitted to further processing stages.

The optical quality of the eye has been measured for centuries, but with the increased availability of wavefront aberrometers, applications have now expanded from basic understanding of the eye's optical quality to the evaluation of aberrations in different eye conditions and corrections (among others, contact lenses or intraocular lenses). However, the processes underlying neural adaptation to ocular aberrations are not yet well understood. Moreover, typically, the impact of ocular aberrations on vision is studied using wavefront sensors with monochromatic, generally infrared, light. However, the retinal image quality is degraded by the presence of both monochromatic and polychromatic aberrations in the ocular optics. Novel polychromatic visual simulators allow the study of the impact of retinal image quality on vision considering both the aberrations in the visible light, as well as the effect of chromatic aberrations.

Adaptive Optics visual simulators, inspired by previous developments for astronomy, are now able to couple the measurement of the aberrations with their correction or manipulation by means of different active technologies (deformable mirrors, spatial light modulators, optotunable lenses working on temporal multiplexing mode). This opens the possibility of performing psychophysics under fully corrected optics, for example projecting identical images on the retina of different observers, providing a patient with the optics of another, or exploring to what extent the eye adapts to its own aberrations and its ability to adapt to low or high order aberrations than its own.

Moreover, optical and structural properties of the eye change with age and with certain ocular conditions and treatments, altering the natural aberrations, as well as the interactions between monochromatic and chromatic aberrations, and consequently the visual function. Very recently visual simulators have proved their capability to map the phase profile of a contact lens or an intraocular lens onto the active elements of an adaptive optics system and explore vision with those corrections prior to being fitted or implanted in the eye, and even manufactured, therefore allowing the patient to experience different corrections in a completely non-invasive manner. The understanding of the interactions of these aberrations and their effect upon correction is essential to explore the limits of human spatial vision, and to design and optimize new alternatives of correction of Presbyopia/Myopia and more complex individualized refractive corrections.

# Part II
# Talks

# Investigation of Thickness Distribution of Magnetron Sputtered Diamond-like Carbon and Silver Nanocomposite by Spectroscopic Ellipsometry

Jurkevičiūtė Aušrinė[1,2,3,*], Dolmantas Paulius[2,3], Tamulevičius Tomas[2,3], Prikulis Juris[1]

[1] *Institute of Chemical Physics, University of Latvia, Jelgavas st. 1, LV-1004, Riga, Latvia*

[2] *Institute of Materials Science of Kaunas University of Technology, K. Baršausko st. 59, LT-51423, Kaunas, Lithuania*

[3] *Department of Physics, Faculty of Mathematics and Natural Sciences, Kaunas University of Technology, Studentu st. 50, LT-51368, Kaunas, Lithuania*

[*] *E-mail:* ausrine.jurkeviciute@lu.lv

Spectroscopic ellipsometry is a non-destructive, high sensitivity technique for investigation of materials optical properties, layer thicknesses, volume concentrations, etc. [1]. It is very convenient as it is not affected by ambient light and intensity fluctuations of light source, and does not require special sample preparation or vacuum conditions [2]. The drawback of the technique is its indirect nature: the desired results are obtained from the fitting of the model to experimental data [3].

In this work, investigation of diamond-like carbon and silver nanocomposite (DLC:Ag) by spectroscopic ellipsometry is presented. Thin film was deposited on silicon substrate by unbalanced magnetron sputtering in direct current mode using silver target. Deposition parameters: 0.1 A current, 366 V voltage, $7.8 \times 10^{-3}$ mbar pressure, 80 sccm argon flow rate, 17.5 sccm acetylene flow rate. Growth time was 1132 s. The sample was measured by GES5-E (Semilab) rotating compensator spectroscopic ellipsometer at 22 spots with 0.5 mm distance between them. Measurements were carried out in reflection mode at 45°-75° incidence angles with the step of 5° with wavelength range of 250-950 nm.

Fitting was done employing *Spectroscopic Ellipsometry Analyzer* (Semilab) software. Optical model of the sample was created taking into account previous experience of modelling nanocomposites [4]. Optical properties of silicon, silver, and air were taken from build-in *n&k* database and DLC was modeled using Cody-Lorentz dispersion law. DLC:Ag mixture was modeled using Maxwell-Garnett effective medium approximation. Simulated Annealing fitting algorithm was employed and the goodness of fit was described by coefficient of determination ($R^2$) and root mean square error (RMSE).

The results showed that the thickness is gradually changing across the sample. With increasing thickness, silver volume concentration is decreasing. It could mean that the actual amount of silver in the nanocomposite is distributed evenly, but the amount if matrix (DLC) increases. In turn, these physical differences result in the change of optical properties.

**References**

[1] C. Zhong, et al. *Journal of the Optical Society of America B* **33** (2016), p. 566.
[2] T. Schram, et al. *Advanced Engineering Materials* **1** (1999), p. 63-66.
[3] M. Gilliot, et al. *Applied Surface Science* **421** (2017), p. 453-459.
[4] A. Jurkevičiūtė, et al. *Thin Solid Films* **630** (2017), p. 48-58.

# Classification of New Atomic Lines of Thulium in the Visible Region using FT Spectroscopy

Parlatan Seyma[1,*], Kanat Ozturk Ipek[2], Basar Gonul [2], Basar Gunay [3], Tamanis Maris [4], Ferber Ruvin [4], Kroger Sophie [5]

[1] *Istinye University, Vocational School of Health Services, TR-34020, Zeytinburnu, Istanbul, Turkey*

[2] *Istanbul University, Faculty of Science, Department of Physics, TR-34134 Vezneciler, Istanbul, Turkey*

[3] *Istanbul Technical University, Faculty of Science and Letters, TR-80626 Maslak, Istanbul, Turkey*

[4] *Laser Centre, The University of Latvia, Rainis Boulevard 19, LV-1586 Riga, Latvia*

[5] *Hochschule für Technik und Wirtschaft Berlin, Wilhelminenhofstr. 75A, D-12459 Berlin, Germany*

[*] *E-mail:* seyma.parlatan@istinye.edu.tr

The aim of this investigation is to provide further spectroscopic data for the element thulium (Tm). Tm belongs to the group of lanthanides and has only one stable isotope, $^{169}$Tm. The nuclear spin of this isotope is I=1/2, consequently only magnetic dipole hyperfine splitting is observed in the spectra. Spectroscopic data of lanthanides are required in particular for astrophysical purposes, as for example for the investigations of so-called peculiar stars. Large overabundances of lanthanides have been observed in these kinds of stars.

Emission spectra of a Tm hollow cathode discharge lamp in the visible wavelength region were measured with a high-resolution Bruker IFS 125 HR FT spectrometer at the Laser Centre of the University of Latvia. The hollow cathode consisted of metallic Tm with a purity of 99.9%. The measurements were carried out with both argon and neon as buffer gas. This enables us to clearly assign spectral lines in the spectrum to the element Tm.

For the analysis of the spectra, we utilized a classification program called Class-LW [1]. As basic input, the program reads the Fourier Transform spectra of the element and a comprehensive list of all experimentally known fine structure levels and hyperfine structure constants. The line classifications were made considering the hyperfine structures of atomic spectral lines ([2] and references therein).

We classified a total of 1757 spectral lines as atomic Tm I out of 2746 lines analyzed. Of these 1757 lines, 289 were classified as Tm I for the first time.

**Acknowledgment**

University of Latvia team acknowledges support from the Latvian Council of Science Project No. lzp-2020/1-0088.

**References**

[1] Windholz, L. and Guthohrlein, G. H., 2003 Phys. Scr., T105, 55.

[2] Basar G., Basar G., Ozturk I.K., Acar F.G. and Kroger S., 2005 Phys. Scr. 71 159.

# Highly sensitive whispering gallery mode humidity sensor

Milgrave Lase[1,*], Reinis Pauls Kristaps[1], Brice Inga[1], Alnis Janis[1], Atvars Aigars[1]

[1] *University of Latvia, Institute of Atomic Physics and Spectroscopy*

[*] *E-mail:* lase.milgrave@lu.lv

Nowadays, demand for sensitive and precise sensors is increasing. Accurate humidity measurements are important in scientific research, industrial environment, museums, and other [1]. To achieve these properties, optical sensors are being researched. In particular whispering gallery mode (WGM) sensors as they offer high Q factors and high sensitivity [2]. Differently shaped resonators are available, sphere being the most common and used in this research.

Microsphere used for the experiments was made of a material sensitive to relative humidity (RH) – glycerol. It is a viscous, transparent, non-toxic, and hygroscopic liquid [3], making it a perfect choice for RH measurements. WGM modes were excited using a 760 nm tunable laser and free-space coupling, which is effective in liquids [4]. Transmission signal was collected by a photodiode and transmitted to an oscilloscope. Modes are visible on screen as dips in the transmission signal. Their corresponding wavelength depends on the radius R and the refractive index n of the droplet. As glycerol absorbs water, it changes its R and n, leading to a change in the resonant wavelength – modes start shifting left (RH decreases) or right (RH increases). Using LabView and an original Python programme, we can detect these changes and use the glycerol droplet as a humidity sensor. Measurements were made in the 50–70 % RH range. Temperature dependence was tested.

Results showed the average sensitivity of 2.85 nm/% RH, higher than previously reported for any type of WGM humidity sensor. Glycerol sphere also showed good temperature independence, high repeatability, and long lifetime.

In conclusion, experiments revealed that a glycerol droplet can be used as a highly sensitive humidity sensor with potential industrial applications. Further research is necessary to create a portative set-up, and to determine the response time.

This study was financed by LZP project Nr.lzp-2018/1-0510 'Whispering gallery mode microresonator sensors'.

**References**

[1] Z. Chen and C. Lu, "Humidity sensors: A review of materials and mechanisms," Sens. Lett., vol. 3, no. 4, pp. 274–295, 2005.

[2] M. Gomilšek, "Whispering gallery modes," Ljubljana, 2011.

[3] G. P. Association, "Physical Properties of Glycerine and its Solutions," 1963.

[4] Y. Wang et al., "A review of droplet resonators: Operation method and application," Opt. Laser Technol., vol. 86, pp. 61–68, 2016.

# Analysis of angular momentum alignment-to-orientation conversion in Rb atoms caused by linearly polarized excitation and an external magnetic field.

Mozers Arturs[1], Busaite Laima[1], Osite Dace[1,*], Auzinsh Marcis[1]
[1] *Laser Centre, University of Latvia, Rainis Boulevard 19, LV-1586 Riga, Latvia*
[*] *E-mail:* dace.osite@gmail.com

Magnetooptical effects in atoms can be used in a variety of applications, for example magnetic sensors [1], optical switches [2] and others. And one such effect dependent on the external magnetic field studied in this research is the angular momentum alignment-to-orientation conversion (AOC).

In general, linearly polarized light can create an alignment parallel (longitudinal alignment) or perpendicular (transverse alignment) to the quantization axis. If the alignment is longitudinal, the magnetic sublevel population for levels $+m_F$ and $-m_F$ is equal. But for transverse alignment there are coherences between $\Delta m_F = 2$ magnetic sublevels. The orientation of angular momentum can be created in a similar way (usually with circularly polarized light). When the angular momentum is orientated along the quantization axis, the $+m_F$ and $-m_F$ sublevels have different populations, however when the orientation is transverse there are coherences between $\Delta m_F = 1$ magnetic sublevels.

In specific conditions the alignment can be converted to orientation. One such perturbation is the joint action of hyperfine interaction and an external magnetic field. This causes an initially aligned state to convert into a partially oriented state.

We created an experiment where these conditions were met. The atoms were excited with a linearly polarized light $\mathbf{E}$ at a $\pi/4$ angle with respect to the external magnetic field $\mathbf{B}$ (quantization axis). The induced hyperfine structure transitions were in the Rb D1 line. The AOC signals were observed as two oppositely circularly polarized fluorescence components in the direction perpendicular to $\mathbf{E}$ and $\mathbf{B}$.

The measured signals show that the maximum 4% level of circularity can be obtained if the laser frequency is fixed to the $F_g = 2 \rightarrow F_e = 2$ transition [3]. Additionally we performed analysis which showed that different velocity groups impact the signals by changing the shapes of and widening the observed signal structures. In some cases the difference signals coming from different velocity groups cancel eachother out, thus leading to the detection of local signal minima. To distinguish which part of the signals came from the ground state and which from the excited state, we simulated signals where the ground-state coherences were eliminated by increasing the relaxation rate of non-diagonal elements in the density matrix.

**References**

[1] D. Budker, W. Gawlik, D. F. Kimball, S. M. Rochester,V. V. Yashchuk, and A. Weis, Resonant nonlinear magneto-optical effects in atoms, Rev. Mod. Phys.74,1153 (2002).
[2] P. Yeh, Dispersive magnetooptic filters, Appl. Opt. 21, 2069 (1982).
[3] A. Mozers, L. Busaite, D. Osite, and M. Auzinsh, Angular momentum alignment-to-orientation conversion inthe ground state of Rb atoms at room temperature, Phys.Rev. A102, 053102 (2020).

# Enhancement of organic compounds luminescence by surface plasmon resonance

Silis Raivis[1,*], Mikelsone Jelena[2], Vembris Aivars[3]
[1] *Institute of Solid State Physics, University of Latvia*
[*] *E-mail:* raivis.silis@cfi.lu.lv

Surface plasmon resonance for metal nanoparticles can enhance the luminescence of organic luminophores, so it can pave the way for the development of light modulators, laboratory chips, or sensors based on organic semiconductors. Within the framework of this study, silver nanoprisms and nanospheres of different sizes were obtained in aqueous solution, which were stabilized with Na citrate and PVP (Polyvinipyrrolidone). Nanoparticles had to be transferred to the organic environment because most luminophores are insoluble in water. This was achieved by two methods: ultrasonic method and the replacement of stabilizers. The obtained nanoparticles in organic media with different concentrations were added to organic luminophore DWK-1-TB solution. Thin films were also obtained from this solution. The quantum yield and the change in luminescence, depending on the type of nanoparticles, were studied in the obtained samples.

**References**

[1] Abhishek P. Kulkarni, Keiko Munechika, Kevin M. Noone, Jessica M. Smith, and David S Langmuir 2009, 25(14), 7932–7939
[2] Qiao Zhang, Na Li, James Goebl, Zhenda Lu, and Yadong Yin, J. Am. Chem. Soc. 2011, 133, 18931–18939, doi: dx.doi.org/10.1021/ja2080345
[3] Alisha Goyal, Jyoti Rozra, Isha Saini, Pawan K Sharma and Annu Sharma, Advanced Materials Research Vol 585 (2012) pp 134-138
[4] Alejandra López-Millán, Paul Zavala-Rivera, Reynaldo Esquivel, Roberto Carrillo, Enrique Alvarez-Ramos, Ramón Moreno-Corral, Roberto Guzmán-Zamudio and Armando Lucero-Acuña, Appl. Sci. 2017, 7, 273; doi:10.3390/app7030273

# Near infrared long persistent luminescence of $CaZnGe_2O_6:Cr^{3+}$ material

Doke Guna[1,*], Krieke Guna[1], Springis Maris[1], Sarakovskis Anatolijs[1]
[1] *Institute of Solid State Physics, University of Latvia*
[*] *E-mail:* guna.doke@cfi.lu.lv

The persistent luminescence (PersL) also called long lasting phosphorescence or afterglow is process characterized by emission of light for a long period of time, usually tens of minutes or more after the removal of the excitation source.

Currently in the literature it is possible to find several hundred combinations of materials and activators that exhibit PersL, however vast majority of studies are devoted to PersL processes in the visible part of the spectrum. Moreover, the ions of rare earth elements are mainly used as activators. In recent years due to their potential application in some advanced fields, such as optical data storage, night-vision surveillance, solar energy utilization, anti-counterfeiting and especially bio-imaging, drug delivery and therapy, considerable attention has been paid to near-infrared (NIR) PersL phosphors [1] [2].

As promising materials for NIR emission trivalent chromium doped gallogermanates and germanates are often mentioned where under the influence of a strong crystalline field $Cr^{3+}$ is typically characterized by emission wavelengths above 700 nm.

In the course of this work $CaZnGe_2O_6$ material doped with 0.5 mol% $Cr^{3+}$ were produced in UL ISSP Laboratory of Spectroscopy using solid-state reaction synthesis.

The sample has undergone a structure study using X-ray diffraction analysis and optical spectroscopy measurements like excitation and emission spectra, thermally stimulated luminescence measurements, luminescence kinetics measurements. We observed photoluminescence and PersL in the spectral region from 700 - 1100 nm as one broad band with a maximum around 820 nm and afterglow time greater than 3 h after excitation with UV.

Based on the obtained experimental results conclusions about the NIR long persistent luminescence processes of $CaZnGe_2O_6:Cr^{3+}$ material will be drawn.

Financial support provided by Scientific Research Project for Students and Young Researchers Nr. SJZS/2019/8 realized at the Institute of Solid State Physics, University of Latvia is greatly acknowledged.

Institute of Solid State Physics, University of Latvia as the Center of Excellence has received funding from the European Union's Horizon 2020 Framework Programme H2020-WIDESPREAD-01-2016-2017-TeamingPhase2 under grant agreement No. 739508, project CAMART$^2$

**References**

[1] Y. Li, M. Gecevicius, J. Qiu, Long persistent phosphors—from fundamentals to applications, Chem. Soc. Rev. 45 (2016) 2090–2136. https://doi.org/10.1039/C5CS00582E.

[2] Y. Liang, F. Liu, Y. Chen, X. Wang, K. Sun, Z. Pan, Extending the applications for lanthanide ions: efficient emitters in short-wave infrared persistent luminescence, J. Mater. Chem. C. 5 (2017) 6488–6492. https://doi.org/10.1039/C7TC01436H.

# Kerr effect experimental value comparison to Quantum Chemical calculations results in organic chromophores

Bundulis Arturs[1,*], Mihailovs Igors[1], Rutkis Martins[1]
[1] *Institute of Solid State Physics, UL*
[*] *E-mail:* arturs@cfi.lu.lv

One of the main building blocks for next generation information and communication technologies will be materials with profound third-order nonlinear optical (NLO) properties to allow for opto-optical interactions. Special interest has been given to organic materials due to their high NLO efficiency. One of the main problems for finding efficient nonlinear optical materials is the slow experimental material screening for applicability. To reduce the amount of experimental work for material selection scientists have long worked to improve Quantum Chemical calculation (QCC) methods to predict hypothetical molecules NLO properties. This could allow to shift most of the material development from experimental to theoretical work by simpler structure screening. Although different QCC methods have already been employed for calculations of NLO properties a systematic comparison between experimental and QCC data is necessary to select most appropriate methods.

In this work we studied third-order NLO properties of multiple organic chromophores using Z-scan method. Z-scan method was chosen as it allows to simultaneously measure Kerr and two-photon absorption effects. Studied molecules were measured in form of solutions by dissolving chromophores in organic solvent. NLO properties were studies using picosecond laser to insure that no thermal effects influenced experimental measurements. Acquired results were compared to QCC carried out with Gaussian 09 and Dalton 2016 software to see how well calculations predict the Kerr effect values. Comparison of experimental and QCC values showed that ratio between both values strongly depend on two-photon absorption values of specific molecule. These results can be further used to adjust calculation methods to better predict experimental results.

**References**

# Manganese doped calcium aluminate luminescent sensing materials

Kemere Meldra[1,*], Rodionovs Pavels[1], Rogulis Uldis[1], Vitols Kaspars[1], Antuzevics Andris[1], Sarakovskis Anatolijs[1], Smite Mara[2]

[1] *Institute of Solid State Physics, Kengaraga 8, Riga, Latvia, LV-1063*

[2] *Light Guide Optics International, Celtniecibas 8, Livani, Latvia, LV-5316*

[*] *E-mail:* meldra.kemere@cfi.lu.lv

The detection of temperature plays a crucial role in industrial production, science, medicine and also everyday life. In many cases, the temperature measurements in harsh, corrosive circumstances or in media exposed to a strong electromagnetic field are needed [1]. In such circumstances, it is recommended to use non-contact optical thermometers. Inorganic maaterials for optical temperature sensors exploiting the temperature dependence of photoluminescence intensity are widely investigated [1]. However, most of the reports are devoted to photoluminescence of rare earth ions. As transition metal ion activators are cheaper and more accessible, it is important to investigate their properties for temperature detection. In the literature, an intensive photoluminescence of manganese ions in calcium aluminates is reported [2].

In this work, various calcium aluminate crystalline phases doped with 0-2 mol% of manganese ions were synthesized using a solid-state reaction method under air and the combustion synthesis method.

The X-ray diffraction and electronic paramagnetic resonance (EPR) measurements of the samples were performed. Photoluminescence excitation and emission measurements at room temperature were done. Temperature dependence of photoluminescence bands of manganese ions were investigated while heating the samples up to 300 °C.

In the prepared samples photoluminescence bands of $Mn^{2+}$ and $Mn^{4+}$ were observed, their relative intensity varied depending on the activator concentration. The spectral position of $Mn^{2+}$ emission band varied in different crystalline phases. EPR spectra revealed that isolated luminescence centres were formed in the samples. Temperature-dependent photoluminescence experiments showed that with the temperature increase, the intensity of $Mn^{4+}$ luminescence strongly decreased, while only slight change of $Mn^{2+}$ emission intensity was seen.

The financial support of ERDF project Nr.1.1.1.1/19/A/020 is greatly acknowledged.

**References**

[1] Q. Wang, et. al., J. Alloys Compd. **850**, 156744 (2021).

[2] J. Park et. al, Ceramics International **39**, S623-S626 (2013).

# Automatic processing of big multispectral data sets and comparison of skin lesion diagnostic parameters

Plorina Emilija Vija[1,*], Lihacova Ilze[1], Cibulska Evija[1]

[1] *University of Latvia, Institute of Atomic Physics and Spectroscopy, Biophotonics Laboratory*

[*] *E-mail:* evplorina@gmail.com

Various non-invasive imaging methods with application in dermatology and dermo-oncology have been developed by research laboratories in the previous decades both in Latvia and around the world. It continues to be a an engaging field of research in part because skin is the largest and most accessible human organ for investigation. However, imaging methods have historically required a trade-off between data quality and data processing time - the higher the quality of the acquired images, the more computer processing power is required to analyze them. With modern processors various steps of image processing can easily be improved and simplified without sacrificing image quality and a large amount of data can be processed in a shorter time.

At University of Latvia, Biophotonics Laboratory various prototypes utilizing multispectral imaging have been developed and a database of around 1400 image data sets of different benign and malignant skin lesions has been gathered. The images were taken using 405nm, 526nm, 663nm and 964nm multispectral illumination [1].

The goal of this study was to create an automatic processing algorithm and data structure so that all available data sets can be processed and classified by diagnosis more quickly. Such a system would then be used to test new proposed diagnostic parameters. The diagnosis was given by dermatologists attending the previous studies and saved in the database along with the imaging data.The effectiveness of the algorithm will be tested by comparing its output for parameters that have been previously tested in the laboratory [1].

This work has been supported by Latvian Council of Science funded project "Skin cancer early diagnostics accuracy improvement by using neural networks" (agreement No: lzp-2018/2-0052) and University of Latvia, Institute of Atomic Physics and Spectroscopy.

**References**

[1] Ilze Lihacova, Katrina Bolochko, Emilija Vija Plorina, Marta Lange, Alexey Lihachev, Dmitrijs Bliznuks, Alexander Derjabo, "A method for skin malformation classification by combining multispectral and skin autofluorescence imaging," Proc. SPIE 10685, Biophotonics: Photonic Solutions for Better Health Care VI, 1068535 (17 May 2018); https://doi.org/10.1117/12.2306203

# Contactless photoplethysmography for examination of cutaneous flowmotions

Aglinska Alise[1], Marcinkevics Zbignevs[1], Rubins Uldis[2], Grabovskis Andris[2]

[1] *Department of Human and Animal Physiology, University of Latvia, Jelgavas str.1, Riga, Latvia, LV-1586*

[2] *Institute of Atomic Physics and Spectroscopy, University of Latvia, Jelgavas str 3, Riga, Latvia, LV-1586*

[*] *E-mail:* aglinska96@gmail.com

Human skin is the largest and non-invasively accessible organ, which can provide diagnostic information on different chronic diseases; therefore its assessment is of great importance to clinicians. Particularly interesting, hence little studied phenomenon is cutaneous flowmotions- quasi-periodic slow oscillations of blood perfusion produced by alterations of vascular tone. The major components of flowmotions are: myogenic (0.05–0.15 Hz), neurogenic (0.02–0.05 Hz) and endothelial (0.0095–0.02 Hz), which reflect the state of regulatory mechanisms. To date flowmotions were investigated using laser Doppler techniques and little is known on potential of contactless plethysmography as a simple and cost effective alternative. The aim of present study was to explore feasibility of imaging photoplethysmography for assessment of cutaneous flowmotions using wavelet transform analyses.

The pilot study comprised seven young (20-30 years) and healthy volunteers. The video of hand dorsal aspect was registered for 20 min by multispectral camera at 540 nm wavelength, 50 fps and photoplethysmography signal computed. The spectrogram and spectral power densities were determined for all three flowmotion spectral bands, and differences revealed by One Way Repeated Measure ANOVA, with post hoc Tukey test.

In the resting conditions consistent flowmotions were obtained as depicted in spectrogram (Fig.1). The spectral power of all three flowmotion components significantly differ ($p<0.001$): myogenic ($0.097\pm0.015$ a.u.), endothelial ($0.157\pm0.022$ a.u.), neurogenic ($0.119\pm0.012$ a.u.), which is in line with recent studies utilizing laser Doppler technique[1]. It is concluded that contactless photoplethysmography with wavelet transform can be utilized for examination of cutaneous flowmotions.

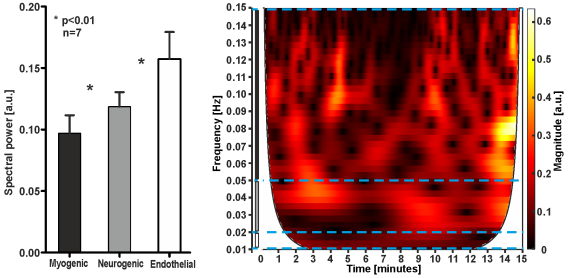


Figure 1: Flowmotion components, group mean±std; Wavelet transform spectrogram

**References**

[1] L.M. Rodrigues, C. Rocha, H. Ferreira. et al., Sci Rep 9, 16951 (2019).

# Fine Structure Analysis in OCT Images for Tumour Tissue Classification

Cizevskis Oskars [1,*], Tamosiunas Mindaugas[1], Viskere Daira [1],Cugmas Blaz[1]

[1] *Institute of Atomic Physics and Spectroscopy, University of Latvia, 19 Rainis Blvd., Riga, LV-1586, Latvia*

[*] *E-mail:* oskars.cizevskis@lu.lv

Spectral domain optical coherence tomography (SD-OCT) allows for non-invasive cross sectional imaging of tissue structure, and thus has a variety of applications in the medical field. However, highly scattering, homogeneous tissue (like those of sarcomas and mast cell tumours) pose a problem, as they are difficult to distinguish from one another by mere visual inspection of the OCT images. Furthermore, SD-OCT imaging has inferior resolution to, say, confocal microscopy [1, 2], and, by design, SD-OCT only produces grayscale images, making diagnosis all the more difficult.

To tackle this issue, simple machine vision techniques were employed to analyse the fine structure of the tissue. Three classes of canine tumours were compared – lipomas, soft tissue sarcomas (STS) and mast cell tumours (MCT). In total, 36 images of STS, 33 of lipoma, and 29 of MCT tissue were taken using Thorlabs Telesto II SD-OCT with a reported axial resolution of 5 $\mu m$.

A $\sim$80x80 $\mu m$ scanning window was used to calculate a distribution of CV values for each image. Given these followed a normal distribution, the mean and standard deviation of CV values sufficiently characterised the data. It was found that lipomas can be distinguished from STS and MCT with at least $2\sigma$ confidence, while means of CV values between STS and MCT were similar. However, the standard deviation was notably larger for STS than that of MCT. These results demonstrate the potential of SD-OCT devices to be used as a non-invasive, quick way to diagnose tumour types, warranting further research into the topic.

**References**

[1] S.-W. Lee et al., "Axial resolution and depth range of high-resolution spectral domain optical coherence tomography at 1.3 $\mu$m," Optical Coherence Tomography and Coherence Domain Optical Methods in Biomedicine XIII, 2009.

[2] C. Fouquet et al., "Improving Axial Resolution in Confocal Microscopy with New High Refractive Index Mounting Media," PLOS ONE, vol. 10, no. 3, 2015.

# In-vivo diagnostics of skin malformations using multimodal RGB imaging

Dambite Laura[1,*], Kuzmina Ilona[1], Oshina Ilze[1], Spigulis Janis[1]

[1] *Institute of Atomic Physics and Spectroscopy, University of Latvia, 19 Rainis Blvd., Riga, LV-1586, Latvia*

[*] *E-mail:* laura.dambite@lu.lv

Suspicious skin malformations such as melanoma and basalioma requires a histological examination that is precise, but invasive. Rapid and non-invasive examinations require a device and an appropriate program that analyzes the malformation. One approach is by calculating skin chromophore concentration values.

In this work, we used a multispectral laser device and multispectral LED device1 for capturing RGB images and skin chromophore mapping. The images were analyzed by a special algorithm2, implemented in MATLAB. Four different approaches based on Beer Lambert's law were used and compared. The first approach included the Beer Lambert's law without any additional coefficients. The second approach additionally included loss and attenuation coefficients and the fraction of light that can be absorbed by the epidermis at a certain wavelength. The third approach included absorption and scattering coefficients and the fourth reduced scattering and absorption coefficients and interlayer reflection coefficient. The concentration of melanin, hemoglobin and oxyhemoglobin were calculated for different types of benign pigmented and vascular skin malformations.

The results showed that it is possible to distinguish different types of malformations by comparing the mean values, however the standard deviations overlaps. The first approach distinguishes hemangiomas quite well by comparing the hemoglobin and oxyhemoglobin values. The third approach showed better results compared to the others due to the largest number of positive concentration values.

Additional measurements of skin malformations including malignant and suspicious malformations are required for further evaluation of the algorithm.

**Acknowledgments**

This work was supported by the ERDF project #1.1.1.1/18/A/132 "Multimodal imaging technology for in-vivo diagnostics of skin malformations".

**References**

[1] J. Spigulis "Multispectral, fluorescent and photoplethysmographic imaging for remote skin assessment," MDPI 17(6), 1165 (2017), doi: 10.3390/s17051165

[2]J. Spigulis, I. Oshina, A. Berzina, A.V. Bykov "Smartphone snapshot mapping of skin chromophores under triple-wavelength laser illumination," Journal of Biomedical Optics 22(9), 091508 (2017), doi: 10.1117/1.JBO.22.9.091508

# Repeatability of Corneal Epithelial Thickness Measurements Using Spectral Domain Optical Coherence Tomography in Normal Eyes

Petrovica Inese[1], Švede Aiga[1]

[1] *University of Latvia, Faculty of Physics, Mathematics and Optometry, Department of Optometry and Vision Science, Riga, Latvia*

[*] *E-mail:* inese.petrovica@gmail.com

**Purpose.** To assess repeatability of central and paracentral measurements of corneal thickness (CT) and epithelial thickness (ET) made by commercially available spectral domain optical coherence tomography (SD-OCT) system (Maestro 3D, Topcon).

**Methods**. In 203 healthy eyes of 102 subjects corneal CT and ET was evaluated at central sector and 8 paracentral zones from 5.0-6.0 mm diameter using SD-OCT Maestro 3D (Topcon) with light source 840 nm SLD, speed of scanning 50 000 A-scan/sec., and axial resolution 6 $\mu$m, lateral resolution 20 $\mu$m. Repeatability was assessed using intra-subject standard deviation (SD), coefficient of variation (CoV), and one-way inter class coefficient (ICC).

**Results**. At the central sector and paracentral zones SD was respectively 2.85 $\mu$m and 7.76-11.41 $\mu$m for CT, 1.86 $\mu$m and 2.71-3.51 $\mu$m for ET. At the central zone CoV (%) 0.54 for CT, 3.85 for ET, as at the paracentral sectors 1.49 – 2.10 for CT, 7.65 – 10.99 for ET. ICC values were high for all CT measurements, moderate for central zone ET measurements and low for ET paracentral sector measurements.

**Conclusions**. OCT produced excellent repeatability at central zone for CT measurements and good at paracentral sectors for CT measurements. Repeatability was moderate at central zone for ET measurements and poor at paracentral zones for ET measurements.

**Key words**

corneal pachymetry maps, epithelial thickness maps, optical coherence tomography.

**References**

# Measurements of the luminance and illuminance of road advertisements in Riga

Volberga Liva [1,*], Ikaunieks Gatis[1], Naumovs Lauris[2], Krumina Gunta [1]

[1] *University of Latvia, Faculty of Physics, Mathematics and Optometry, Department of Optometry and Vision Science*

[2] *The Latvian State Roads*

[*] *E-mail:* livavolberga@gmail.com

With the development of the technology of LED large size billboards have come to our roads and towns. These billboards are usually large, have high luminance, show dynamically changing images [1] and affect the drivers' visual performance [2], so road safety. The luminance of billboard should be limited during the night due to the high luminance billboards with low ambient lighting can cause glare for drivers [1]. In the questionnaire study, half of the participants indicated being distracted at least once by roadside advertising signs. Moreover, 22% of them have been in a dangerous situation due to the distraction caused by such signs [2]. Billboards near roads are a potential threat to traffic safety [3].

The study aimed to identify the situation in Riga where more and more digital advertising appears and to assess the measurements of luminance and illuminance for digital billboards. SpectraScan PR-655 spectroradiometer was used for luminance measurements, and Konica Minolta T-10 lux meter – for illuminance measurements. During the dark hours of the day, we performed measurements for white (255, 255, 255) red (255, 0, 0), green (0, 255, 0), blue (0, 0, 255), yellow (255, 255, 0), and grey (125, 125, 125) colours in agreement with the advertising owners.

The measured luminance average value ± SD for different colours where: white colour 210±126, red 76±45, green 115±69, blue 18±11, yellow 190±114, and grey 31±18 cd/m$^2$. The measured illuminance average value ± SD where: white colour 14±7, red 6±2, green 8±4, blue 2±1, yellow 12±6 and grey 4±1 lx.

The Regulation of the Cabinet of Ministers No.402, point 3.2 prescribes that roadside advertising signs shall not dazzle drivers, but there is no normative value for billboards maximal luminance. There is no common approach in the world, and every country has different luminance values and guidelines. Our measurements provide an opportunity to understand the current situation in the country until stricter restrictions will be introduced.

**References**

[1] Domke, K., Wandachowisc, K., Zalesinska, M., Mroczowska, S., & Skrzypczak, P. (2011). Digital Billboards and Road Safety. WIT Transactions on The Built Environment, 121, 119-131.

[2] Bendak, S., & Al-Saleh, K. (2010). The Role of Roadside Advertising Signs in Distracting Drivers. International Journal of Industrial Ergonomics, 40(3), 233-236.

[3] Domke, K., Wandachowisc, K., Zalesinska, M., Mroczowska, S., & Skrzypczak, P. (2012). Large-Sized Digital Billboards Hazard. International Journal of Design and Nature Ecodynamics, 7(4), 367-380.

# Gaze parameters in visual search on the volumetric display

Krauze Linda[1], Konosonoka Vita[1], Pladere Tatjana[1], Krumina Gunta[1]
[1] *Department of Optometry and Vision Science, Faculty of Physics, Mathematics and Optometry, University of Latvia, Riga, Latvia*
[*] *E-mail:* linda.krauze@lu.lv

As eye movements vary depending on the attributes of images [1, 2], eye tracking can be used to assess the user experience for the novel displays. In this study, it has been described for the first time how the spatial layout of elements on the volumetric multi-plane display affects the way images are viewed.

Participants performed visual search tasks on the volumetric multi-plane display. Search elements were presented at four field eccentricities (2, 4, 6, and 8 deg). In target-present trials, the task was to determine which of the four circles was displayed closer to the observer. In target-absent trials, the individuals were instructed to report that images were two-dimensional.

As a result, the correct response rates differed significantly when comparing target-present and target-absent trials. Moreover, the analysis of eye movements revealed that gaze was more often directed to the target when search elements were presented relatively close to each other. However, as the field eccentricity increased, a similar amount of time was devoted to viewing each element on the display.

To conclude, the study showed that it was easier to distinguish three-dimensional images than two-dimensional images on the volumetric multi-plane display. Moreover, as the field eccentricity of the elements increased, the distribution of fixations changed indicating that it was more difficult to evaluate the relative depth of elements in the optical element of the volumetric-multi-plane display.

This work is a part of the research project "Evaluation of volumetric display's 3D image effect on human visual system", No. ZD2019/20807. It was supported by the European Regional Development Fund ("Development of a compact, high-brightness laser image projection system for application in volumetric 3D displays", project No. 1.1.1.1/18/A/179).

**References**

[1] Staugaard, C. F., Petersen, A., Vangkilde, S. Eccentricity effects in vision and attention. Neuropsychologia, 2016, 92, pp. 69-78.

[2] Yu, J. H., Lee, B., Kim, D. EOG based eye movement measure of visual fatigue caused by 2D and 3D displays, Proceedings of IEEE-EMBS International Conference on Biomedical and Health Informatics, 2012, pp. 305-308.

# Twelve-Year Prospective Audit of LASIK Outcomes for Myopia patients

Jansone-Langina Zane [1,*], Gertnere Jana[2], Bogdanova Lasma[2], Truksa Renars[1], Solomatins Igors[2]

[1] *University of Latvia, Faculty of Physics, Mathematics and Optometry, Optometry and Vision Science department, Riga, Latvia*

[2] *Dr. Solomatina Eye rehabilitation and vision correction centre, Riga, Latvia*

[*] *E-mail:* jansonezane1993@gmail.com

Background. Refractive surgery is mostly performed on young and healthy eyes of patients with high expectation and long-term safety and efficacy is the biggest concern. However, there is little knowledge about the general changes in visual acuity, refractive tendencies, and the anatomic parameter stability of patients without post-operative problems stability.[1] Our aim was to assess and evaluate the long-term clinical outcomes of laser in situ keratomileusis (LASIK) for myopia patients in 12-year period.

Methods. In our research we evaluated 60 preoperative myopic eyes (mean spherical equivalent (SE) of $-5,91 \pm 2,54$D) treated with LASIK. Patient data were separated in three groups divided by myopic grade – low (11 eyes), moderate (23 eyes), high (26 eyes). All patients were evaluated one day, three months, one year, five years, ten to twelve. The main outcome measures were objective refractive power, subjective refraction, uncorrected (UCVA) and best corrected visual acuity (BCVA), central corneal pachymetry and axial length.

Results. Low grade myopia eyes subjective refractive power increased for $+0,28 \pm 0,26$ D, objective for $-0,39 \pm 0,36$ D. UCVA reduced by $-0,20 \pm 0,15$ decimal units, BCVA by $-0,12 \pm 0,22$ decimal units. Corneal thickness changed by $6,22 \pm 13,03$ $\mu$m, axial length $0,01 \pm 0,05$ mm. Moderated eyes UCVA reduced by $-0,31 \pm ,34$ decimal units (mean UCVA $0,77 \pm 0,33$ decimal units), BCVA decreased by $-0,01 \pm 0,10$ decimal units (mean BCVA twelve years after the surgery $0,99 \pm 0,11$ decimal units). The mean corneal pachymetry change was $5,60 \pm 17,12$ $\mu$m). Axial length increased for $0,06 \pm 0,04$ mm. 12 years after LASIK surgery preoperative high grade myopic eyes mean UCVA was $0,32 \pm 0,30$ decimal units, with a correction of $0,85 \pm 0,15$ decimal units. UCVA change was $-0,63 \pm 0,29$ decimal units, BCVA $-0,09 \pm 0,13$ decimal units. The corneal thickness changed for $18,02 \pm 25,42$ $\mu$m, axial length $0,20 \pm 0,26$mm.

Conclusion. Low and moderated grade myopia eyes do not show statistically significant difference (p¡0,05) in UCVA, BCVA, subjective and objective refraction power twelve years after LASIK surgery. High grade myopia progresses during lifetime due axial length growth, corneal thickness thickening and showed statistical significance in all the parameters.[2]

**References**

[1] Lim, S., A., Park, Y., Cheong, Y., J., Na, S., K., Joo, C., K. (2016) Factors Affecting Long-term Myopic Regression after Laser In Situ Keratomileusis and Laser-assisted Subepithelial Keratectomy for Moderate Myopia, Korean J Ophthalmol.30, 2, 92-100

[2] Ide, T., Toda, I., Fukumoto, T., Watanabe, J., Tsubota, K.(2014) Outcome of a 10-year follow-up of laser in situ laser keratomileusis for myopia and myopic astigmatism, Taiwan Journal of Ophthalmology, 4, 4, 156-162

# Part III
# Poster Session 1

# Dispersion engineering of whispering gallery mode resonators for Kerr frequency comb generation

Draguns Kristians[1]

[1] *AFFOC Solutions Ltd., 17 Andrejostas street, 1045 Riga, Latvia*
[2] *Institute of Atomic Physics and Spectroscopy, University of Latvia, 3 Jelgavas street, 1004 Riga, Latvia*
[*] *E-mail:* kristians.draguns@gmail.com

Whispering gallery mode resonators (WGMRs) are optical devices with axial symmetry, where light is propagating along the perimeter of the resonator due to total internal reflection. WGMRs are around 10 – 1000 $\mu$m large, and they experience strong light-matter interaction due to low losses and low mode volume. WGMRs can be used to generate Kerr Frequency combs by inducing four-wave mixing [1]. The Kerr frequency combs are generated at anomalous dispersion and it is good to have a flat dispersion profile for best results. Thus it is important to engineer the resonator to achieve the desired results [2]. For telecommunication applications, the desired free spectral range is around 100 GHz, which occurs in a WGMR radius of 332 $\mu$m [3]. An interesting geometry is disk type WGMR, where the dispersion profile can be achieved quite flat. The disk resonators are cylindrical structures with its side a triangular side. Computer simulations are made in COMSOL Multiphysics to determine the dispersion. For telecommunication applications, the pumping laser should be somewhere in the middle of the C-band region (1530 nm – 1565 nm).

**References**

[1] Chembo, Y. K. (2016). Kerr optical frequency combs: Theory, applications and perspectives. Nanophotonics, 5(2), 214–230.

[2] Fujii, S., & Tanabe, T. (2020). Dispersion engineering and measurement of whispering gallery mode microresonator for Kerr frequency comb generation. Nanophotonics, 9(5).

[3] E.A. Anashkina, M.P. Marisova, A. V. Andrianov, R.A. Akhmedzhanov, R. Murnieks, M.D. Tokman, L. Skladova, I. V. Oladyshkin, T. Salgals, I.Lyashuk, A. Sorokin, S. Spolitis, G. Leuchs, V. Bobrovs, (2020). Microsphere-based optical frequency comb generator for 200 GHz spaced WDM datatransmission system, Photonics. 7.

# Harmonic and anharmonic approximation for ZPVE calculation. Analysis based on the example of hydrogen peroxide molecule

Khrapunova Aryna[1], Kisuryna Darya[1,*], Shender Dmitry[1], Malevich Alex[1], Pitsevich George[1]

[1] *Faculty of Physics, Belarusian State University, Minsk, Belarus*

[*] *E-mail:* kisurinadasha@gmail.com

The analysis of the large-amplitude motions in molecules and compounds remains one of the most interesting and non-trivial sections of molecular spectroscopy today. Among several types of motions with a large amplitude the most interesting case is probably the internal rotation of individual fragments of a molecule with respect to the molecular frame. Since in this case the values of the torsion coordinates that describe the internal rotation can take all possible values, it is necessary to calculate the dependence of the kinetic parameters and potential energy on the given torsion coordinates and then to numerically solve the vibrational Schrödinger equation with a restricted dimensionality [1].

However, recently, publications in which the dependence of zero point vibrational energy on torsion coordinates is additionally taken into account when calculating multidimensional potential energy surfaces started to appear. This beautiful idea, however, requires both theoretical foundation and practical confirmation of the effectiveness in performing calculations of the energy of stationary torsion states of molecules in which internal rotation is realized.

In this paper, the second problem was solved. As a touchstone, we used the hydrogen peroxide ($H_2O_2$) molecule for which vast experimental data on torsional-rotational IR spectra is presented in papers. The energy of stationary torsion states was calculated in three ways: 1) without taking into account the energy of zero vibrations, 2) taking into account zero point vibrational energy calculated in the harmonic approximation, 3) taking into account zero point vibrational energy calculated in the anharmonic approximation. All calculations were performed at the MP2/acc-pVQZ theory level. The graph of dependence of zero point vibrational energy on torsional angle is shown in Fig. 1.

Additionally, the possibility of scaling of zero point vibrational energy calculated in harmonic approximation for partially taking into account the effects of anharmonisity was analyzed.

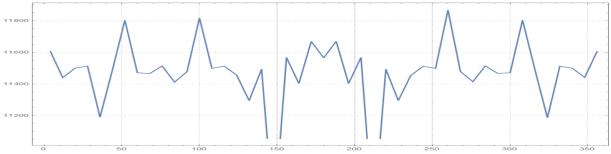


Figure 1: Dependence of zero point vibrational energy of the hydrogen peroxide molecule on the torsional angle $\theta$.

**References**

[1] G.A. Pitsevich, A.E. Malevich, U.U. Sapeshka, Chem.Phys., 530 (2020) 110633

# High resolution spectroscopy of hyperfine structure of the first triplet state in KCs

Krumins Valts[1], Kruzins Artis[1], Tamanis Maris[1,*], Ferber Ruvin[1], Pashov Asen[2], Stolyarov Andrey[3]

[1] *Laser Center, Faculty of Physics, Mathematics and Optometry, University of Latvia, 19 Rainis blvd, Riga LV-1586, Latvia*

[2] *Faculty of Physics, Sofia University, 5 James Bourchier blvd., 1164 Sofia, Bulgaria*

[3] *Department of Chemistry, Moscow State University, 119991 Moscow, Leninskie gory 1/3, Russia*

[*] *E-mail:* maris.tamanis@lu.lv

We have performed high resolution Fourier-transform spectroscopy studies of the laser induced fluorescence (LIF) transitions to the first triplet $a^3\Sigma^+$ state of KCs. Due to the hyperfine structure (hfs) in the $a^3\Sigma^+$ state, each rotational line consists of three groups, see Fig. 1. Splitting between the groups reflects strong coupling of molecular spin **S** (S = 1) with the nuclear spin $\mathbf{I}_{Cs}$ (I = 7/2) of Cs atom. The resultant moment **G**1 is coupled with nuclear spin $\mathbf{I}_K$(I = 3/2) of K atom, producing moment **G**2, and then **G**2 is coupled with the rotational moment **N** yielding 96 hfs components. Since magnetic dipole interaction with $\mathbf{I}_K$ is much weaker than with the one of Cs, the hfs components within the groups are not resolved in the experiment. Though most of theoretical models, which describe the hfs in $a^3\Sigma^+$ state, assume that magnetic dipole interaction is not dependent on the internuclear distance R, see e.g. [1], recent theoretical analysis for KCs [2] predicts weak dependence on R, or on vibration level $v_a$ of the $a^3\Sigma^+$ state. In order to check the estimates of [2], we have recorded LIF transitions to the $a^3\Sigma^+$ state with ultra-high resolution (0.0063 $cm^{-1}$) and found that the splitting between right (r) and left (l) hfs groups is increasing with $v_a$, see Fig. 2. The quantitative analysis of measurements is in progress.

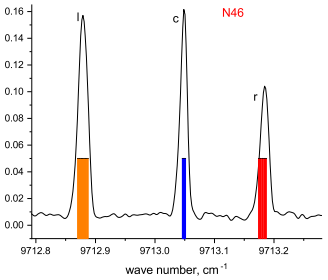


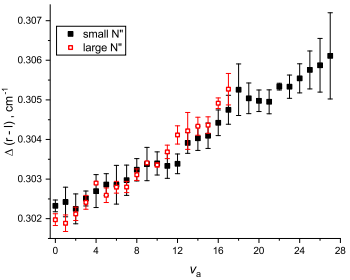


We acknowledge support from the Latvian Council of Science Project No. lzp-2020/2-0215.

**References**

[1] R. Ferber et. al. *Phys. Rev.* **A80**, 062501 (2009).

[2] A. V. Oleynichenko et. al. *Chem. Phys. Lett.* **756**, 137825 (2020).

# A systematic study of the mixed $A^1\Sigma_u^+$ and $b^3\Pi_u$ states in $K_2$: experiment and deperturbation treatment

Klincare Ilze[1,*], Brakmane Ieva[1], Lapins Adams[1], Kruzins Artis[1], Tamanis Maris[1], Ferber Ruvin[1], Stolyarov Andrey [2], Pazyuk Elena[2]

[1] *Laser Center, Faculty of Physics, Mathematics and Optometry, University of Latvia, 19 Rainis blvd, Riga, Latvia LV-1586,*

[2] *Department of Chemistry, Moscow State University, 119991 Moscow, Leninskie gory 1/3, Russia*

[*] *E-mail:* ilze.klincare@lu.lv

The following considerations motivate the present study of the mixed $A^1\Sigma_u^+$ - $b^3\Pi_u$ states in $K_2$. As already mentioned in [1], over significant energy region the term values data are rather sparse and involve only the $^{39}K^{39}K$ isotopomer. As a result the existing deperturbation treatment [1] does is not applicable to the full range of experimental data, see [2]. So, there is hope that addressing these issues may allow providing the description of the $A^1\Sigma_u^+$ - $b^3\Pi_u$ states in $K_2$, which will reproduce the term values with the experimental accuracy, that is, within 0.01 $cm^{-1}$ uncertainty, or better. To reach this goal, we aimed to considerably increase the amount and abundance of accurate term value data, also to include the data for $^{39}K^{41}K$ and$^{41}K^{41}K$ isotopologues. We performed in the University of Latvia Laser Center in Riga the rotationally resolved Fourier-transform spectroscopy measurements of $A^1\Sigma_u^+ - b^3\Pi_u \rightarrow X^1\Sigma_g^+$ laser-induced fluorescence (LIF) applying a Ti:sapphire laser and various diode lasers. The collision-induced population of rotational levels $J'$ of the excited state made it possible to obtain the considerably increased amount of data systematically spanned over $J$ values. Fig. 1 presents LIF spectrum recorded at excitation of $K_2$ with laser frequency 11625.54 $cm^{-1}$. Strongest doublet progression (blue points) originates from the level with rotational quantum number $J' = 57$, $E' = 12029.423$ $cm^{-1}$. The red points mark progression from collisionally populated neighbor level with $J' = 57$, $E' = 12031.265$ $cm^{-1}$. The present data field, see Fig. 2, contains about 4300 term values for $^{39}K^{39}K$ and 730 term values for $^{41}K^{39}K$ (blue points), which systematically cover large energy range spanning over $J'$ range from 3 to 160. The 4x4 coupled-channel depeturbation treatment has been performed yielding empirical potential parameters and spin-orbit interaction functions. We acknowledge

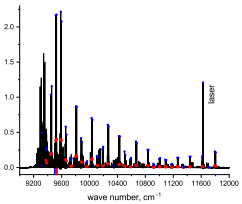


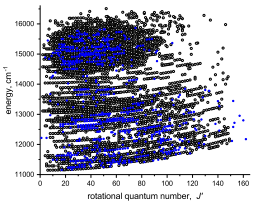


support from the Latvian Council of Science Project No. lzp-2018/1-0020.

**References**

[1] M.R. Manaa et al, *J. Chem. Phys.*, **117**, 11208 (2002).

[2] St. Falke et al, *J. Chem. Phys.*, **125**, 224303 (2006).

# ZnO-based nanostructures for the development of label free optical immunosensors

Tereshchenko Alla[1,*], Konup Igor[1], Smyntyna Valentyn[1]
[1] *Odesa National I.I. Mechnikov University*
[*] *E-mail:* alla_teresc@onu.edu.ua

The thin films based on ZnO nanostructures have been intensively used as a template for biosensors due to their fundamental physico-chemical properties such as the direct wide band gap (Eg 3.37 eV) semiconductor complemented by a high surface-to-volume ratio of its nanostructures being chemically stable. ZnO has a high isoelectric point (pH 9–9.5), good biocompatibility and affinity towards proteins along with strong adsorption ability that make it suitable for the immobilization of various protein-based immune complexes applied as biological recognition part in immunosensors [1]. Excellent optical properties of ZnO, in particular, an intense room temperature photoluminescence open a great possibility to be used for optical biosensor applications. Recently, a range of photoluminescence-based immunosensors based on ZnO nanostructures have been developed [1,2]. Regarding to a progress in nanotechnology and material science, new technological methods have been developed to fabricate nanostructured ZnO templates with high surface area and advanced properties for biosensors, e.g. atomic layer deposition (ALD) [3], metal organic chemical vapor deposition (MOCVD) [4] and others. In this report, the influence of immobilized proteins of the immune complex on the photoluminescence spectra of ZnO thin films will be demonstrated. The potential applications of ZnO-modified substrates for the development of other label free immunosensors based on immobilized antibodies sensitive to selected analyte will be discussed.

**References**

[1] A. Tereshchenko, M. Bechelany, R. Viter, et.al., Sensors and Actuators B, Chemical 229, 664 (2016).
[2] R. Viter, A. Tereshchenko, V. Smyntyna, et.al., Sensors and Actuators B: Chemical, 252, 95 (2017).
[3] A. Tereshchenko, V. Fedorenko, V. Smyntyna, et.al., Biosensors and Bioelectronics 92, 763 (2017).
[4] A. Tereshchenko, G. R. Yazdi, I. Konup, et.al., Colloids and Surfaces B: Biointerfaces 191, 110999 (2020)

# Persistent luminescence of $Cr^{3+}$doped $MgGeO_3$

Kalnina Aija[1,*], Doke Guna [1]

[1] *Institute of Solid State Physics, University of Latvia*

[*] *E-mail:* aija@cfi.lu.lv

Persistent luminescence has wide range applications from science to practical life, luminophores are used in light sources, bioluminescent markers, electronics and so on. Persistent luminescence has been studied in the blue and green spectral regions, however much less research has been devoted to the red and infrared part of the spectrum, which is useable in medicine [1]. One of the materials that can provide persistent afterglow in the red and near-infrared spectral range with the appropriate impurities is $MgGeO_3$. There are few publications on the luminescence properties of this material, most often describing $MgGeO_3$ activated with $Mn^{2+}$ ions. Long afterglow in the red and infrared range in different matrices is also provided by $Cr^{3+}$ impurity ions.

In the course of this study $MgGeO_3$:$Cr^{3+}$ samples with $Cr^{3+}$ concentration of 0 mol %, 0.1 mol %, 0.25 mol %, 0.5 mol %, 0.75 mol %, 1 mol %, 2 mol % and 5 mol % were prepared by high temperature solid state reaction. The luminescent properties of $MgGeO_3$:$Cr^{3+}$ samples were investigated by X-ray diffraction, thermally stimulated luminescence spectra, excitation and emission spectra, afterglow spectra etc. Material excited by X-rays or UV exhibit intense infrared luminescence with a peak around 780 nm. Examination of the afterglow spectra shows that after excitation samples continues to glow at least 48 hours. Based on obtained results, conclusions about $MgGeO_3$:$Cr^{3+}$ material luminescence has been drawn.

**References**

[1] Y. Liu and B. Lei, "Persistent Luminescent Materials," in Phosphors, Up Conversion Nano Particles, Quantum Dots and Their Applications, Singapore: Springer Singapore, 2016, pp. 167–214.

# Neural indicators of cognitive load when working with the volumetric multi-plane display

Naderi Mehrdad[1,*], Pladere Tatjana[1], Krumina Gunta[1]

[1] *Department of Optometry and Vision Science, Faculty of Physics, Mathematics and Optometry, University of Latvia, Jelgavas 1, Riga, Latvia, LV-1004*

[*] *E-mail:* mehrdad.naderi@lu.lv

The development of three-dimensional visualization technologies requires the comprehensive assessment of human factors. Cognitive load has been broadly studied in visual neuroscience allowing to describe mental states during information processing and learning [1, 2]. This study aimed to assess the potential indicators of cognitive load when individuals were completing visual tasks on the volumetric multi-plane display. All subjects were divided into two groups: first-timers (performed the visual search task on the volumetric display for the first time) and familiar users (performed the same task several times). The recorded brain signals were analyzed to compare the event-related potential (P300) and continuous brain oscillations in theta, alpha and beta frequency bands which could serve as indicators of the cognitive load. The results showed the average latency of the P300 component was longer in first-timers compared to others. Moreover, differences were revealed in the power of theta and beta waves, but not in that of alpha frequency band, although differences did not reach the statistical significance. To sum up, it was shown that the assessment of brain activity might allow to track the learning process when working with the novel display. The work is a part of the research project "Evaluation of volumetric display's 3D image effect on human visual system", No. ZD2019/20807. It was supported by the European Regional Development Fund ("Development of a compact, high-brightness laser image projection system for application in volumetric 3D displays", project No. 1.1.1.1/18/A/179).

**References**

[1] [1]Dan, A., Reiner, M. (2017). Real time EEG based measurements of cognitive load indicates mental states during learning. JEDM Journal of Educational Data Mining, 9(2), 31-44.

[2] [2]Dan, A., Reiner, M. (2017). EEG-based cognitive load of processing events in 3D virtual worlds is lower than processing events in 2D displays. International Journal of Psychophysiology, 122, 75-84.

# Eccentric fixation training in amblyopia

Kalnica-Dorosenko Kristine[1,2,*], Svede Aiga[1]
[1] *University of Latvia, Department of Optometry and Vision Science (Riga, Latvia)*
[2] *Children's Clinical University Hospital, Eye Diseases Clinic (Riga, Latvia)*
[*] *E-mail:* kristinekalnica@gmail.com

Amblyopia is diminished vision that results from inadequate visual experience during the first years of life [1]. Eccentric fixation in amblyopia occurs when there is a long-term decrease or loss of central visual acuity in the amblyopic eye. Eccentric fixation is present in around 44 % of all patients with amblyopia and in 30 % of patients with strabismic amblyopia [2]. The angle of fixation can serve as a preliminary determinant of the severity of amblyopia, i.e., the larger it is, the more severe the degree of amblyopia [2]. In Latvia, amblyopia is carefully treated in various clinics, but eccentricity diagnosis is relatively rare. A case report: a 5-year-old boy with a congenital haemangioma on the left side of his face was unable to open his left eye for the first 2-3 weeks of his life because of a formation in the orbit. Received liquid propranolol therapy for up to 1 year, after which the formation decreased significantly. Right eye occlusions were prescribed, but which he only started actively doing from the age of 4 to 5. The boy also has strabismus – exotropia 20 $\Delta$ BI with hypotropia 10 $\Delta$ BD of the left eye. VEP and OCT examinations show no abnormalities. Other pertinent findings included: steady central fixation of the right eye and unsteady 6 $\Delta$ temporal eccentric fixation of the left eye. Visual acuity has gone from 0.05 to 0.2 (in decimal units) in the left eye in 1.5 years and is no longer improving. Afterwards, eccentric fixation training in the amblyopic eye of a child was suggested once a week, using macula integrity tester (MIT). So far the training has been effective and the first positive results are noticeable.

**References**

[1] Birch, E.E. (2013). Amblyopia and binocular vision. Prog Retin Eye Res, 33, 67-84.
[2] von Noorden, G.K. (1970). Etiology and pathogenesis of fixation anomalies in strabismus. I. Relationship between eccentric fixation and anomalous retinal correspondence. Am J Ophthalmol, 69(2): 210-222.

# Computerized colour arrangement test applications in optometrist practice

Polupanova Anastasija[1,*], Truksa Renars[1], Jansone-Langina Zane[1], Fomins Sergejs[1]

[1] *Department of Optometry and Vision Science, Faculty of Physics, Mathematics, and Optometry, University of Latvia, Riga, Latvia*

[*] *E-mail:* anastasijapolupanova@gmail.com

In optometric practice colour vision tests are used for screening purposes, i.e., to detect whenever person has colour vision deficiency. Most of colour vision tests like Isihihara, HRR, D15 saturated and unsaturated versions used by optometrists, do not enable optometrists accurately diagnose type and severity of colour vision deficiency, and do not provide means to assess chromatic sensitivity changes due to diabetes, glaucoma and other systemic and eye diseases.

Anomaloscope test is used to unequivocally diagnose type and severity of congenital red-green colour vision deficiencies, however tests like Isihihara provide almost equivalent accuracy of congenital red-green colour vision screening for fraction of anomaloscope price and unfortunately conventional anomaloscope tests cannot be used to evaluate blue-yellow colour vision because of significant differences of short wavelength part absorption properties in crystalline lens and macular pigment among general population.

Colour arrangement test FM100 could be suggested as optimal solution, which could provide adequate colour vision screening and evaluation of chromatic sensitivity changes due to diseases, physiological ageing processes. We have designed computer program to overcome inherited colour arrangement test problems, i.e., physical FM-100 tests colour cap illuminance fluctuations and complex scoring algorithm.

During our research we will test validity of computerized colour arrangement test in comparison to physical colour arrangement test in three age groups 40-50, 50-60, 60-70 years of age at two different illumination levels (24 and 60 cd/m2). We expect to confirm that computerized version will provide comparable results to FM100 physical test version and enable assessment of light absorption effects within crystalline lens and macular pigment on colour discrimination.

In conclusion, this research results in near future can provide optometrists with relatively simple and accessible method to enable diagnosis of acquired and congenital colour vision deficiencies in optometrist practices.

**References**

# Part IV
# Poster Session 2

# Studies of the $c^3\Sigma^+$ state in KCs based on Fourier-Transform spectroscopy data

Krumins Valts[1], Kruzins Artis[1], Tamanis Maris[1], Ferber Ruvin[1,*], Brakmane Ieva[1], Lapins Adams[1], Stolyarov Andrey[2]

[1] *Laser Center, Faculty of Physics, Mathematics and Optometry, University of Latvia, 19 Rainis blvd, Riga LV-1586, Latvia*

[2] *Department of Chemistry, Moscow State University, 119991 Moscow, Leninskie gory 1/3, Russia*

[*] *E-mail:* ruvins.ferbers@lu.lv

Laser induced fluorescence (LIF) spectra of the $c^3\Sigma^+ \rightarrow a^3\Sigma^+$ transition ($c \rightarrow a$ in short) of KCs molecule were recorded with Fourier-Transform spectrometer IFS125-HR (Bruker) using InGaAs detector. Spectral resolution was set as 0.03 cm$^{-1}$. KCs molecules were produced in a linear heat-pipe at about 300$^o$C. The Ti:Saphire laser Equinox/SolsTis (MSquared) operated within 13800 - 12900 cm$^{-1}$ range was exploited and $c \rightarrow a$ LIF signal was recorded in the spectral range from 9000 to 10 000 cm$^{-1}$. Assignment of the $c \rightarrow a$ progressions was based on the $a^3\Sigma^+$ potential energy curve (PEC) obtained in [1] and measured rotational-vibrational differences. The upper state vibrational numbering was proved by comparison of experimental and theoretical relative LIF intensity distribution, see Fig. 1. We obtained a set of about 750 new term values with increased accuracy of about 0.01 cm$^{-1}$, which are covering enlarged range of rotational quantum numbers and extended to higher vibrational levels than in [2], see Fig. 2. The obtained data have been used for construction of the effective empirical potential of the $c^3\Sigma^+$ state.

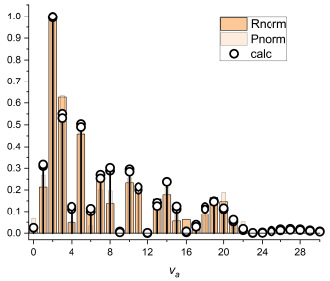


Figure 1: LIF $c^3\Sigma^+ \rightarrow a^3\Sigma^+$ relative intensity distribution from excited state vibrational level $v'$=23, and rotational level $N'$=26; bars - experiment, circles - calculations.

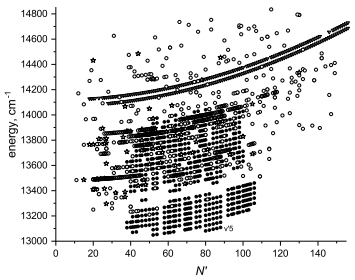


Figure 2: The $c^3\Sigma^+$ state term values as dependent on $N'$: empty circles - $e$ levels, stars - $f$ levels, points - data from [2], triangles - $B^1\Pi$ data.

We acknowledge support from the Latvian Council of Science Project No. lzp-2018/1-0020.

**References**

[1] R. Ferber et. al. *Phys. Rev.* **A80**, 062501 (2009).

[2] J. Szczepkowski et.al *JQSRT*, **204**, 131-7 (2018).

# Determination of short-range repulsive interatomic potential of KCs above the $a^3\Sigma^+$ state dissociation limit

Krumins Valts[1,*], Kruzins Artis[1], Tamanis Maris[1], Ferber Ruvin[1], Stolyarov Andrey[2], Pazyuk Elena[2]

[1] *Laser Center, Faculty of Physics, Mathematics and Optometry, University of Latvia, 19 Rainis blvd, Riga LV-1586, Latvia*

[2] *Department of Chemistry, Moscow State University, 119991 Moscow, Leninskie gory 1/3, Russia*

[*] *E-mail:* valts.krumins@lu.lv

Experiment-based construction of short-range repulsive part of ground singlet and triplet states can serve for testing models of quantum chemical calculations and will help for theoretical predictions of the transport processes, including diffusion coefficients, in the environment of alkali metal atoms. The short-range part of interatomic potential can be obtained from observations of bound-free radiative transitions to the repulsive part of the potential above dissociation limit. Given well known excited electronic state, from which transitions originate, character of the intensity distribution of the continuous fluorescence signal depends on wave functions of the upper and lower states and the electric transition dipole moment [1]. In present study we report on determination of repulsive part of the ground triplet $a^3\Sigma^+$ state of KCs above the dissociation limit based on detection and analysis of oscillation structure of $c^3\Sigma^+ \rightarrow a^3\Sigma^+$ transitions in LIF spectra recorded with Fourier transform spectrometer in near-infra-red range with InGaAs detector, see Fig. 1. The Ti:Saphire laser Msquare/Soltis operating in frequency range 13 000 – 13 800 cm$^{-1}$ was used for $c^3\Sigma^+ \rightarrow a^3\Sigma^+$ LIF excitation. Assignment of LIF progressions $v'$, $N' \rightarrow v''$, $N'' = N' \pm 1$, where $v$, $N$ are vibrational and rotational quantum numbers respectively, was based on the $a^3\Sigma^+$ state potential from [2, 3]. In Fig.1 the LIF spectrum from the level $v' = 27$, $N' = 48$ with oscillating intensity in bound - free transition range is presented. The potential used for spectrum simulation (red curve in Fig.1) is presented in Fig. 2, see dotted curve, along with previous potentials from Refs. [2, 3].

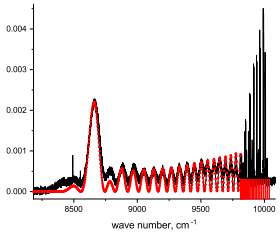


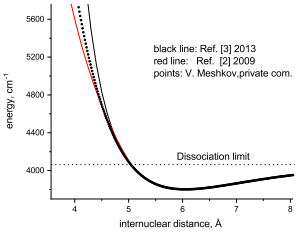


We acknowledge support from the Latvian Council of Science Project No. lzp-2020/2-0215.

**References**

[1] H. Lefebvre-Brion and R. W. Field, The Spectra and Dynamics of Diatomic Molecules, Academic Press, New York (2004).

[2] R. Ferber et. al. *Phys. Rev.* **A80**, 062501 (2009).

[3] R. Ferber et. al. *Phys. Rev.* **A88**, 012516 (2013).

# Ab initio Fock-space Coupled Cluster study of the RaF molecule promising for laser cooling

Osika Yuliya[1,*], Shundalau Maksim[1]

[1] *Faculty of Physics, Belarusian State University, Belarus*

[*] *E-mail:* yulia.osika@gmail.com

The unique properties of ultracold diatomic molecules can be applied in different fields such as the creation of the molecular Bose-Einstein condensate, quantum information processing and precision measurements [1]. One of the possibilities of obtaining molecular quantum matter with controlled properties is the transferring of the polar diatomic molecules to the ground rovibronic state by initial optical excitation into the overlying rovibronic states. In this case for the high efficiency of excitation and subsequent relaxation of the molecular system, the exact forms of the potential energy curves (PECs) of the combining electronic states can be obtained based on analysis and interpretation of high-resolution rovibronic spectra or cutting-edge *ab initio* calculations. The knowledge of the exact PECs also allows defining the important spectra-energetic characteristics of molecules and the macroscopic physical properties of rarefied gases.

Recently [2, 3], it was shown that radium fluoride RaF is a promising candidate for direct laser cooling in order to use it for measuring molecular parity violation. According to the ab initio FS-CCSD calculations [3], the equilibrium internuclear distances for the ground and first excited states of the RaF molecule almost coincide, which provides high values of the diagonal FCFs.

In this study, *ab initio* state-of-art calculations at the FS-CCSD level of the theory of the low-lying potential energy curves of the RaF molecule were performed for the first time. The calculated PECs are shown in Fig. 1.

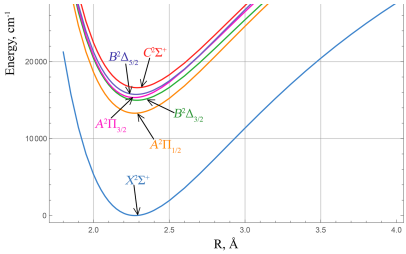


Figure 1: The PECs of the low-lying doublet states of the RaF molecule.

The spectroscopic parameters were calculated for the following low-lying RaF terms: ground state $X^2\Sigma^+$, and excited states $A^2\Pi_{1/2}$ ($T_e = 13298$ cm$^{-1}$), $B^2\Delta_{3/2}$ ($T_e = 14988$ cm$^{-1}$), $A^2\Pi_{3/2}$ ($T_e = 15332$ cm$^{-1}$), $B^2\Delta_{5/2}$ ($T_e = 15745$ cm$^{-1}$), and $C^2\Sigma^+$ ($T_e = 16628$ cm$^{-1}$). The results of our calculations are in excellent agreement with experimental values [2].

*This work was supported by State Scientific Research Program "Convergence-2025".*

**References**

[1] O. Dulieu, C. Gabbanini. Rep. Prog. Phys. 72, 086401 (2009).
[2] R.F. Garcia Ruiz et al. Nature 581, 396 (2020).
[3] T.A. Isaev, S. Hoekstra, R. Berger. Phys. Rev. A 82, 052521 (2010).

# Studies of short-range repulsive interatomic potential of KCs above the $X^1\Sigma^+$ state dissociation limit

Kruzins Artis[1], Klincare Ilze[1], Tamanis Maris[1,*], Ferber Ruvin[1], Stolyarov Andrey[2], Pazyuk Elena[2]

[1] *Laser Center, University of Latvia, 19 Rainis blvd, Riga LV-1586, Latvia*

[2] *Department of Chemistry, Moscow State University, 119991 Moscow, Leninskie gory 1/3, Russia*

[*] *E-mail:* tamanis@latnet.lv

In present work we report on study of the repulsive part of the ground singlet $X^1\Sigma^+$ state potential of the KCs molecule above the dissociation limit. This short-range repulsive part of interatomic potential can be reconstructed from observations of bound-free radiative transitions. In the experiment the laser-induced fluorescence (LIF) spectra of the continuous bound-free transitions $(4)^1\Sigma^+ \rightarrow X^1\Sigma^+$ were recorded with a Fourier-transform spectrometer. The $(4)^1\Sigma^+$ state has been studied in detail in [1,2], hence, its properties are well known, including the radiative transition dipole moment function. According to Ref. [2] the bound-free transitions from the $(4)^1\Sigma^+$ state can be observed at excitation of high vibrational levels, $v' > 44$. Selected rovibronic $v'$, $J'$ levels of the $(4)^1\Sigma^+$ state have been excited with cw single-mode dye laser Coherent 699-21. In order to achieve the required contrast of the bound-free LIF signal the rotational levels with low rotational quantum number $J'$ were excited. Special attention was paid to maintain selectivity of excitation in order to minimize an undesired contribution from other levels into LIF signal. Examples of recorded bound-free transitions are presented in Fig. 1 and Fig. 2. The dotted vertical bars in the figures mark transitions from the excited levels to bound part of the $X^1\Sigma^+$ state. The study is under progress.

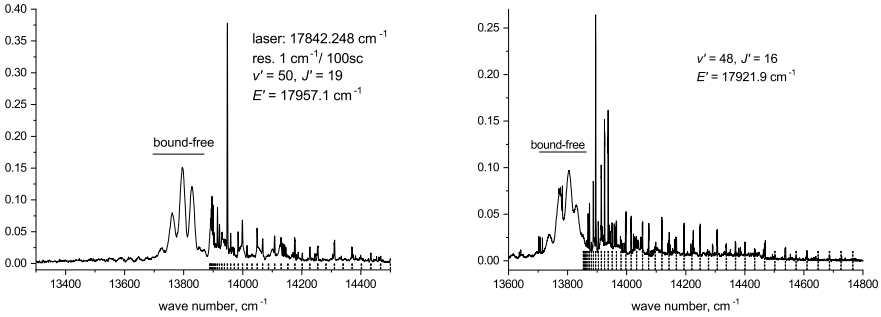


We acknowledge support from the Latvian Council of Science Project No. lzp-2020/2-0215.

**References**

[1] L. Busevica et.al. *J. Chem. Phys.* **134**, 104307 (2011).

[2] I. Klincare et. al. *Phys. Rev. A* **85**, 062520 (2012).

# Hot carriers in a single junction solar cell

Masalskyi Oleksandr [1,*], Gradauskas Jonas[1]

[1] *Vilnius Gediminas Technical University*

[*] *E-mail:* oleksandr.masalskyi@vilniustech.lt

The investigation is based on the assumption that photons having energy larger than a semiconductor forbidden energy gap as well as photons having energy smaller than the gap need to be accounted through the hot carrier phenomena participating in the photoresponse formation in solar cells before the lattice gets heated.

In general, the photoresponse of a solar cell consists of three components. First, $U_G$, is the classical electron-hole pair generation-caused one. Second, $U_{HC}$, is hot carrier photovoltage induced across a p–n junction and it has polarity opposite to $U_G$. Third, $U_T$, is the thermalization component; it is slower than $U_{HC}$, has the same polarity and is caused by subsequent heating of the lattice [1]. Thus, hot carrier phenomena opposes the classical photovoltage and this way reduces the conversion efficiency of solar cells [1,2].

In the experimental part, GaAs p-n-junction was illuminated with 25 ns-long laser pulses of 1.06 $\mu$m wavelength. Short enough pulse and the wavelength opened a way to demonstrate experimentally presence of hot carrier photoresponse and its direct impact on the net photovoltage.

In the theoretical part, we have created a model allowing to separate photoresponse signal of three components mentioned above. The model assumes that a p-n solar cell can be described as the first-order linear time-invariant system and lets purifying individual input of each component. Thus, the finding opens the way to reveal the conditions determining their contribution into the net photovoltage signal. The proposed model shows good agreement with the experimental results.

These results may be valuable for the PV community in two ways: first, they show that creating of conditions unfavorable for the rise of hot carrier photovoltage might improve the efficiency of a single junction solar cell, and second, it may invoke the reason to revise the Shockley-Queisser limit [3] by taking into account the hot carrier phenomena.

**References**

[1] J. Gradauskas, S. Asmontas, et al., Unfolding hot carrier impact in photovoltage across a p-n junction, Appl. Sci. 10, 1-8 (2020).

[2] S. Asmontas, L. Fedorenko, et al., Suppression of hot carriers by nanoporous silicon for improved operation of a solar cell, Ukr. J. Phys. Opt. 21, 207-214 (2020).

[3] W. Shockley and H. J. Queisser, Detailed balance limit of efficiency of p–n junction solar cells, J. Appl. Phys. 32, 510-519 (1961).

# Optical and electroluminescence properties of solution processed Ir(ppy)3 derivatives in different hosts

Tetervenoka Natalija[1], Traskovskis Kaspars [2], Vembris Aivars [1]

[1] *Institute of Solid State Physics, University of Latvia, 8 Kengaraga Street, Riga LV-1063, Latvia*

[2] *Riga Technical University, Faculty of Materials Science and Applied Chemistry, 3/7 Paula Valdena Street, Riga LV-1048, Latvia*

[*] *E-mail:* natalie@cfi.lu.lv

Organic light emitting diodes (OLEDs) are nowadays treated as the most convenient technological approach for superior quality displays [1]. Due to high costs of vacuum deposition, wet processible compounds for OLEDs are being investigated.

Among plenty of investigated compounds that are applicable for solution processing, Ir(ppy)3 (tris(2-phenylpyridine)iridium) stands out by reason of its noteworthy thermal and chemical stability and high photoluminescence quantum yield ($\phi$PL) of near 1.0 [2]. Comparing to vacuum deposition, when its $\phi$PL maintains near a unity, aggregation of Ir(ppy)3 appears during solution processing, which results in phase separation between the emitter and host material [3]. This process leads to a reduction of OLEDs efficiency. To avoid this condition, it has been found out that adding bulky groups with charge transport or purely isolating functionality to Ir(ppy)3 core ensures a physical barrier that helps to retain a sufficient distance between emitter molecules and suppresses the tendency of aggregate formation.

In this study Ir(ppy)3 core was supplemented with a gradually increasing number of passive isolating groups. The molecular composition of these compounds consists of Ir(ppy)3 core and one (1TPY), two (2TPY) or three (3TPY) attached bulky triphenylmethane groups (TR). Optical properties of Ir(ppy)3 and its structural analogues were investigated. There were not observed significant deviations in absorption and emission spectra among all compounds, which means that adding TR groups does not notably affect the electronic configuration of Ir(ppy)3 core.

Afterwards, series of corresponding OLEDs with a solution-processed emissive layer using hole deficient, electron deficient or balanced host material were made and analyzed. Using the balanced host material showed the best result in the sense of turn-on voltage, current and power efficiencies and maximal brightness.

Researched compounds provide an opportunity to use them as emitters in solution-processable OLEDs, but additional studies are required.

**References**

[1] Chen, H.W., Lee, J.H., Lin, B.Y., Chen, S. and Wu, S.T., 2018. Liquid crystal display and organic light-emitting diode display: present status and future perspectives. Light: Science & Applications, 7(3), pp.17168-17168.

[2] Baldo, M., Lamansky, S., Burrows, P., Thompson, M. and Forrest, S., 1999. Very high-efficiency green organic light-emitting devices based on electrophosphorescence. Applied Physics Letters, 75(1), pp.4-6.

[3] Kim, Y.T., Seol, J.B., Kim, Y.H., Ahn, H.J. and Park, C.G., 2017. Correlation of Controllable Aggregation with Light-Emitting Property in Polymer Blend Optoelectronic Devices. small, 13(14), p.1602874.

# Computerized vision screening for school-aged children

Slabcova Jelena[1,*], Krumina Gunta[1]
[1] *University of Latvia, Department of Optometry and Vision Science (Riga, Latvia)*
[*] *E-mail:* jelena.slabcova@lu.lv

Relevance. During school years, children experience a lot of stress factors for their visual system – reading, writing, using computers and other digital devices [1]. This huge load of visual system, which requires precise focusing and fixation of the very close viewing distance, often exceeds the child's physiological abilities and results with inappropriate work of accommodation and vergence system [2]. In turn, undetected vision problems can cause of reduction of academic achievement performance [1].

Purpose. The research aim is to develop modified computerized screening model to assess near vision problems in school-aged children.

Method. Globally, there is a lack of standardized school vision screening programs [3]. Therefore, we evaluate previously developed computerized screening model by our department (82% sensitivity, 71% specificity) and created its modification.

Results. Modified computerized screening model has synchronized additional filters and pairs of lenses using during the different tests and are mounted on the head helmet glasses. Some of tests and stimuli were modified to improve screening model sensitivity and specificity. Now, screening model includes tests for visual acuity at distance, hyperopia, accommodation facility, suppression and stereovision, heterophoria and AC/A, vergence facility and amplitude, colour vision. This screening model doesn't require additional staff.

Conclusion. Currently, the modified computerized vision screener is being approbated under laboratory conditions. This screener should be easy to use, cost-effective and good alternative to the manual screening model.

Acknowledgment The research is based on project No. KC-PI-2020/10 "Development of vision screening and training equipment".

**References**

[1] Falkenberg, H.K., Langaas, T., & Svarverud, E. (2019). Vision status of children aged 7–15 years referred from school vision screening in Norway during 2003–2013: a retrospective study. BMC Ophthalmology, 19, article No180.
[2] Podugolnikova, T.A., Shubina, M.O., & Cherkasova, E.V. (2014). Visual Screening For Elementary School Children: A pilot research. New Research, 2(39), 41-51.
[3] Metsing, I.T., Hansraj, R., Jacobs, W., & Nel, E.W. (2018). Review of school vision screening guidelines. African Vision and Eye Health, 77(1), article No 444.

# Wavelength measuring using PMMA WGM micro resonator and image analysis methods.

Berkis Roberts[1], Draguns Kristians[1], Alnis Janis[1], Brice Inga[1] , Atvars Aigars
[1] *Institute of Atomic Physics and Spectroscopy, University of Latvia, 3 Jelgavas street, 1004 Riga, Latvia*
[*] *E-mail:* robertsberkis2007@inbox.lv

Poly methyl methacrylate acrylic (PMMA) WGM micro resonators are available with quality factor of $10^3$-$10^4$ [1] ,while the Q factor is lower than WGM made from SiO2 or ZnO [2] ,they are available commercially , solving the main problem for successful WGM micro resonator integration into working sensor system , that is the manufacturing cost.

Using high resolution cameras , such as ''Xenics Xs-5049" it is possible to monitor individual sectors of the micro resonator (see Fig.1) and watch each sector intensity changes , based on the wavelength , that is fed to tapered fibber.

From each specific region of the micro resonator, normalized intensity map can be obtained (see Fig.2), which can be used to navigate specific wavelength. Each region intensity corresponds to different mode interaction with impurities on the WGM PMMA micro resonator surface.

The following work presents, new type of measuring system, where two main regular problems, that tie with WGM micro resonators – surface impurities and multiple modes, that lead to system improvements where few PMMA WGM micro resonators can be used as an measuring tool for telecommunication purpose [3]. These developed methods are valid not only for wavelength measuring but could be used for different bio measurements as well.

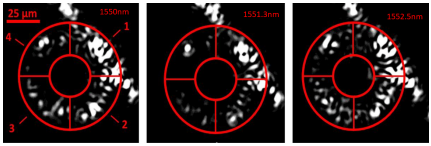


Figure 1: 45$\mu$m PMMA WGM micro resonator attached to tapered fibber waist region, intensity using ''Xenics Xs-5049" camera, for different wavelengths (1550nm , 1551.3nm and 1552.5nm).

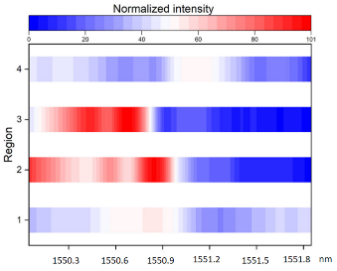


Figure 2: Normalized intensity map based on wavelength changes for 50$\mu$m PMMA WGM micro resonator.

**Acknowlegments** This research was funded by the Latvian Council of Science project No. lzp-2018/1-0510: "Optical whispering gallery mode microresonator sensors" and ERDF 1.1.1.5/19/A/003 project No. 1.1.1.5/19/A/003 "The Development of Quantum Optics and Photonics in University of Latvia".

**References**

[1] R. Berkis et al, IEEE 9th Int. Conf. Nanomater. Appl. Prop. N. 2019 9–12 (2019).
[2] A. E. Shitikov et al, Optica 5, 1525 (2018).
[3] A. B. Petermann et al, Sensors Actuators, A Phys. 252, 82–88 (2016).

ISBN 978-9934-23-356-2


SPIE. STUDENT CHAPTER UNIVERSITY OF LATVIA

OSA University of Latvia Student Chapter

UNIVERSITY OF LATVIA